Nucl. Phys. A 1043 (2024) 122830

Contents lists available at ScienceDirect

Nuclear Physics A

journal homepage: www.elsevier.com/locate/nuclphysa

State dependence of tunneling processes and thermonuclear fusion

Roberto Onofrio [a,*], Carlo Presilla [b,c]

[a] Department of Physics and Astronomy, Dartmouth College, 6127 Wilder Laboratory, Hanover, NH 03755, USA
[b] Dipartimento di Matematica, Sapienza Università di Roma, Piazzale Aldo Moro 2, Roma 00185, Italy
[c] Istituto Nazionale di Fisica Nucleare, Sezione di Roma 1, Roma 00185, Italy

ARTICLE INFO

Keywords:
Quantum tunneling
Nuclear fusion
Statistical mechanics

ABSTRACT

We discuss the sensitivity of tunneling processes to the initial preparation of the quantum state. We compare the case of Gaussian wave packets of different positional variances using a generalized Woods-Saxon potential for which analytical expressions of the tunneling coefficients are available. Using realistic parameters for barrier potentials we find that the usual plane wave approximation underestimates fusion reactivities by an order of magnitude in a range of temperatures of practical relevance for controlled energy production.

1. Introduction

Tunneling processes are of crucial relevance to a broad range of physical systems, including semiconductors [1] and heterostructures [2], α-radioactivity and nuclear fusion in stars [3–5], the early Universe [6], and nuclear fusion processes in the laboratory [7–10]. Apart from an early contribution [11], tunneling probabilities have been usually evaluated by considering incoming plane waves. However in realistic settings as the ones mentioned above, the particles undergoing tunneling cannot in general be fully described by plane waves, either because particles are confined in space, or because in a many-body setting they undergo scattering with other particles, thereby limiting the coherence length of the plane wave [12]. Moreover, there are discrepancies between theoretical expectations and data from fusion experiments [13], and therefore it may be important to scrutinize all the underlying theoretical assumptions.

It is therefore important to discuss the robustness of tunneling coefficients and fusion reactivities with respect to the choice of more general initial states, for instance by considering the representative set of Gaussian wave packets. The use of generalized Gaussian wave packets has been already pioneered by Dodonov and collaborators [14–17], with results confirming that the predictions on tunneling rates may differ even orders of magnitude with respect to the one arising from the Wentzel-Kramer-Brillouin (WKB) approximation usually employed for fusion reactivites. These studies, in particular [16], have been focused on analytical expressions valid under specific conditions, not necessarily encompassing the entire parameter space.

The main goal of the present paper is to extend the above results evaluating the tunneling coefficient for arbitrary values of the position and momentum spreading. The analysis is carried out having in mind applications to high-temperature ionized gases such as light nuclei plasmas in magnetically confined setups. Fusion experiments with heavy-ion beams share the needs to incorporate the role of the energy width using a description in terms of wave packets [18,19]. A key ingredient of our discussion is the use of a potential admitting exact solutions for the tunneling coefficient in the entire energy range. This allows us to pinpoint differences arising from the sole structure of the incoming Gaussian wave packets, excluding other sources of differences as the ones due to the

* Corresponding author.
E-mail addresses: onofrior@gmail.com (R. Onofrio), carlo.presilla@uniroma1.it (C. Presilla).

https://doi.org/10.1016/j.nuclphysa.2024.122830
Received 14 November 2023; Accepted 8 January 2024

Available online 10 January 2024

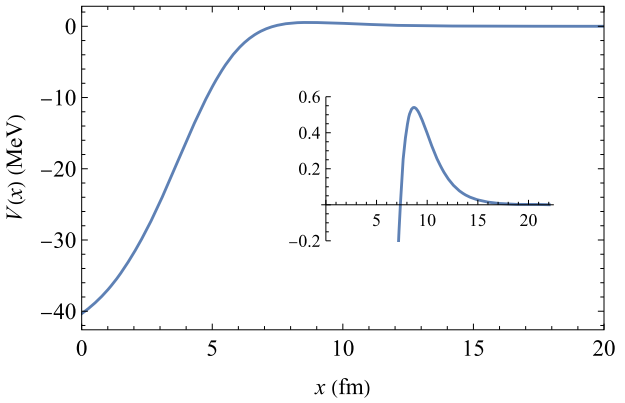

Fig. 1. Positive abscissa plot of the symmetric Generalized Woods-Saxon potential [20] experienced between two nuclei, with parameters $a = 0.6\ \mathrm{fm}^{-1}$, $L = 5$ fm, $V_0 = 45$ MeV, and $W_0 = 56$ MeV. With these parameters the barrier height (from zero to the maximum positive value of $V(x)$) is 0.540 MeV, the well width and depth are 7.35 fm and 40.336 MeV, respectively. All following figures are obtained using these parameters. The inset (vertical units in MeV, horizontal units in fm) allows to better identify the shape of the barrier otherwise barely visible on the broader scale of the well depth.

use of approximations in the calculating techniques. Additionally, we provide more intuitive arguments for the behavior of fusion reactivity in both the cases of very narrow and very broad positional variances. We finally identify optimal operating temperatures for which reactivity gains with the corresponding wave packet states occur with respect to the case of plane wave states.

2. Tunneling from wave packet states

We focus the attention on the Generalized Woods-Saxon (GWS) potential energy for a one-dimensional system first introduced in [20] (see also [21] for a simpler treatment)

$$V(x) = -\frac{V_0}{1+e^{a(|x|-L)}} + \frac{W_0 e^{a(|x|-L)}}{(1+e^{a(|x|-L)})^2}, \tag{1}$$

where both V_0 and W_0 determine the peak values of the potential energy, and L, a, as in the usual Woods-Saxon potential, determine, respectively, the size of the effective well around the origin and its spatial spread. For a convenient choice of these four parameters, the GWS potential represents a symmetric well with value in the origin equal to $-V_0/(1+\exp(-aL)) + W_0\exp(-aL)/(1+\exp(-aL))^2$, and $-V_0/2 + W_0/4$ at $|x| = L$. At large distances $|x| \gg L$ the potential energy decreases exponentially to zero as $V(x) \simeq (W_0 - V_0)\exp(-ax)$, *i.e.*, within a range $\lambda \simeq 1/a$. This means that a semiqualitative difference from potential energies of interest for instance in nuclear fusion is that the barrier experienced by the nucleons, if schematized with this potential, does not have the long range as expected for Coulomb interactions, though in a realistic plasma the latter are screened on the Debye length. In light of the simplicity of the potential capturing the essential feature of the tunneling process, and the presence of exact solutions, we do not expect the results being qualitatively different from the ones achievable by more sophisticated analyses. We choose the set of parameters as described in the caption of Fig. 1, resulting in well depth, barrier height and width of the well comparable to the ones of light nuclei. We do not consider here the effect on tunneling of intrinsic degrees of freedom, such as vibrational or rotational couplings among the nucleons generating excited states, see [22], therefore focusing only of the dependence of fusion rates on the external - due to translational motion - state. Using this potential and the related solutions in terms of tunneling coefficients $T(E)$ evaluated for plane waves at energy E, we have considered more general cases of wave localized in both space and momentum. The most practical case, though not exhaustive of all possibilities, is a Gaussian wave packet.

Let us consider the scattering of a one-dimensional Gaussian wave packet with positional variance ξ^2, characteristic wave vector K and mean energy $\hbar^2K^2/(2m)$. The corresponding wavefunction reads

$$\psi(x) = \left(\frac{2}{\pi\xi^2}\right)^{1/4} e^{-(x-x_0)^2/\xi^2 + iKx}, \tag{2}$$

which in wave vector space k becomes

$$\begin{aligned}\varphi(k) &= \frac{1}{\sqrt{2\pi}}\int_{-\infty}^{+\infty}\psi(x)e^{-ikx}dx \\ &= \frac{1}{(2\pi)^{1/4}}\sqrt{\xi}e^{-\xi^2(k-K)^2/4}e^{i(K-k)x}.\end{aligned} \tag{3}$$

This equation shows that we are dealing with an ensemble of plane waves with wave vector $k \in (-\infty, +\infty)$ distributed according to the probability density

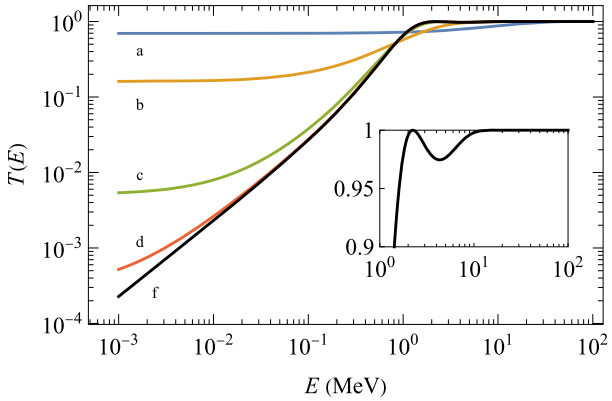

Fig. 2. Transmission coefficient of a Gaussian wave packet of width ξ and mean energy E impinging on the GWS potential of Fig. 1. Curves from a to d respectively correspond to the cases $\xi = 2, 8, 32, 128$ fm, while the case of tunneling of a plane wave f is also depicted. In the inset we show a zoom-in of curve f on the region close to complete transmission, clearly showing one resonant tunneling oscillation. Note that this oscillation is progressively smeared out in curves d-a by decreasing ξ.

$$P(k,K) = |\varphi(k)|^2 = \frac{\xi}{\sqrt{2\pi}} e^{-\xi^2(k-K)^2/2}, \tag{4}$$

where we have introduced the positional spreading ξ as the square root of the positional variance. Note that the probability density $P(k,K)$ is a Gaussian function of $k-K$, i.e., it depends on the mean energy $\hbar^2K^2/(2m)$ of the packet via its characteristic wave vector K.

3. Fusion reactivities from thermal states

The characteristic wave vector K around which the wave vectors of the packet are distributed according to quantum mechanical probabilities is in turn distributed according to the initial classical preparation of the particle's energies. Equation (4) allows us to consider fusion processes taking place in an ensemble of nuclei represented by Gaussian wave packets with arbitrary distribution of their mean energy. In particular, apart from the case of a monoenergetic distribution, or a highly peaked one, therefore represented by a single or a narrow range of K values, respectively – as typically realized in fusion experiments with ion beams – it is important to consider a Maxwell-Boltzmann energy distribution of the particles when modelizing thermonuclear fusion. This translates into considering the convolution of the k wave vectors quantum mechanical distribution and the K characteristic wave vector classical distribution, reminiscent of the Voigt profile broadly used in atomic spectroscopy [23,24]. Therefore we now assume that the nuclei are at thermal canonical equilibrium with inverse temperature β. The one-dimensional wave vector K is then distributed according to the Maxwell-Boltzmann probability density

$$w(K,\beta)_{MB} = \left(\frac{\beta}{\pi}\frac{\hbar^2}{2m}\right)^{1/2} e^{-\beta\hbar^2K^2/(2m)}, \tag{5}$$

where $m = m_a m_b/(m_a+m_b)$ is the reduced mass of the two nuclei a and b which actually take part in the fusion process. Eq. (5), in which the wave vector K can assume any positive or negative value, is normalized as

$$1 = \int_{-\infty}^{+\infty} w(K,\beta)_{MB}\, dK.$$

The spread of the wave vector K is determined by the inverse temperature β, as customary for canonical ensembles.

Particularly relevant to the discussion of fusion processes is the reactivity defined as $\langle\sigma(E)v(E)\rangle_{MB}$ where $\langle\ldots\rangle_{MB}$ denotes the average over the statistical distribution of the reactants, which in our case is the Maxwell-Boltzmann distribution, $\sigma(E)$ is the cross-section of the process, and $v(E)$ is the particle velocity. In one dimension and for nuclei at energy $E = mv^2/2 = \hbar^2k^2/(2m)$, the cross-section is $\sigma(E) = T(E)\pi/k^2$ [25], and

$$\sigma(E)v(E) = \frac{\pi\hbar^2}{\sqrt{2m^3}}\frac{1}{\sqrt{E}}T(E). \tag{6}$$

In our case, each nucleus does not correspond to a monochromatic plane wave at energy $E = \hbar^2k^2/(2m)$, instead it is represented by a Gaussian wave packet with wave vectors k distributed with probability density $P(k,K)$. In turn, the Gaussian wave packets representing the nuclei in the thermal ensemble have characteristic wave vectors K spread with Maxwell-Boltzmann distribution $w(K,\beta)_{MB}$. It follows that the average fusion reactivity is

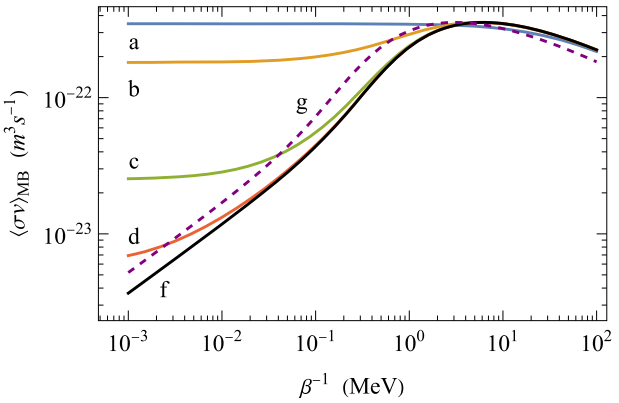

Fig. 3. Fusion reactivity, evaluated for the same Gaussian wave packets of Fig. 2 (and same labeling a-f) with energy E averaged over a Maxwell-Boltzmann distribution as a function of the temperature β^{-1}. The dashed line (case g) is the case in which the positional spreading depends on temperature as $\xi = \lambda(\beta)/\sqrt{2}$, where $\lambda(\beta)$ is the thermal wavelength of the nuclei [26]. The ratio between this latter curve and the curve for a plane wave (case f) versus β^{-1} is reported in the inset to evidence their differences in a region of interest for nuclear fusion.

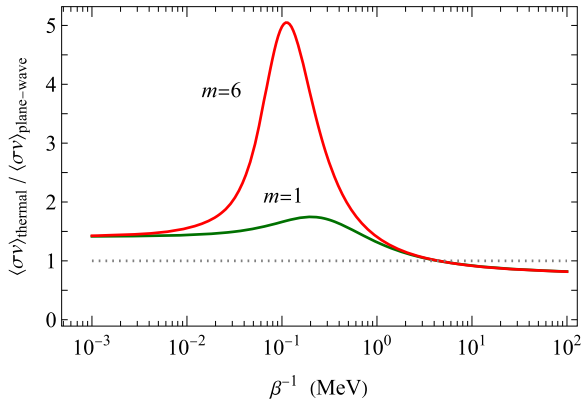

Fig. 4. Enhancement of fusion reactivity with thermal wave packets. The ratio between the dashed line (case g in Fig. 3) in which the positional spreading depends on temperature as $\xi = \lambda(\beta)/\sqrt{2}$, where $\lambda(\beta)$ is the thermal wavelength of the nuclei [26], and the curve for a plane wave (case f in Fig. 3), is reported versus β^{-1} in a temperature region of interest for nuclear fusion. Two cases allow to evidence the dependence of the enhancement on the reduced mass of the nuclei.

$$\langle\sigma v\rangle_{MB} = \frac{\pi\hbar^2}{\sqrt{2m^3}} \int_{-\infty}^{+\infty} dk \int_{-\infty}^{+\infty} dK \left(\frac{\hbar^2 k^2}{2m}\right)^{-1/2} \times T\left(\frac{\hbar^2 k^2}{2m}\right) P(k,K) w(K,\beta)_{MB}. \tag{7}$$

Due to the Gaussian nature of the functions $P(k,K)$ and $w(K,\beta)_{MB}$, the integral over K can be evaluated analytically, yielding the rather compact formula

$$\langle\sigma v\rangle_{MB} = \frac{\sqrt{\pi}}{2}\frac{\hbar}{m} \int_{-\infty}^{+\infty} dk \frac{1}{k} T\left(\frac{\hbar^2 k^2}{2m}\right) \xi_{\rm eff}\, e^{-\xi_{\rm eff}^2 k^2/2}, \tag{8}$$

where we have introduced an effective positional spreading $\xi_{\rm eff}$, depending on the inverse temperature, such that

$$\frac{1}{\xi_{\rm eff}^2} = \frac{1}{\xi^2} + \frac{m}{\beta\hbar^2}. \tag{9}$$

States approximating a plane wave satisfy $\xi^2 \gg \beta\hbar^2/m$, therefore $\xi_{\rm eff}^2 \simeq \beta\hbar^2/m$, i.e., $\xi_{\rm eff}$ becomes the thermal De Broglie wavelength. In the opposite limit of states highly localized in position, $\xi^2 \ll \beta\hbar^2/m$, we have $\xi_{\rm eff} \simeq \xi$. High-temperature Boltzmann states are then approximating wave vector eigenstates (of eigenvalue K), while low-temperature Boltzmann states approximate position eigenstates. This shows that even assuming an initial quantum state with positional variance of quantum nature, at temperature large enough the relevant lengthscale below which quantum coherence of the wave packet is maintained no longer depends on the initial preparation.

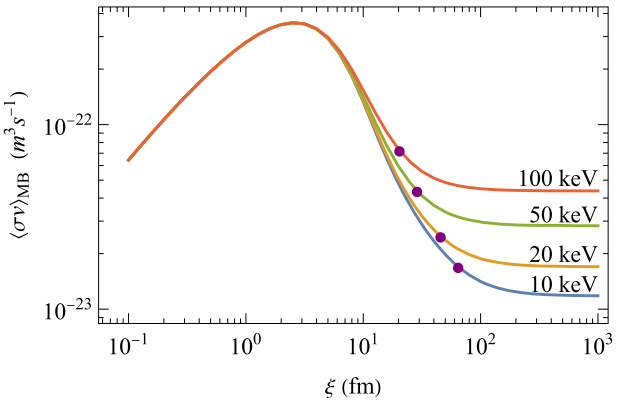

Fig. 5. Fusion reactivity versus the positional spreading ξ for four temperature values $\beta^{-1} = 10, 20, 50, 100$ keV of relevance in fusion of light nuclei. The dots denote the reactivities for the positional spreading from the thermal wavelength of the nuclei as discussed in Fig. 3 and evaluated at the corresponding temperatures shown here.

Analogous conclusions have been already obtained in [26,27]. This can also be interpreted, in the case of a gas at given temperature and density, as corresponding to the mean free path for two-particle collisions.

The tunneling coefficient versus the mean energy of the wave packet E is depicted in Fig. 2 for various values of the width ξ of the Gaussian wave packet. The dependence of the tunneling coefficient on E is, quite predictably, mild when the value of E is comparable or higher than the barrier height. Instead its dependence at lower energies strongly depends on ξ, with the case of plane waves (in the limit of $\xi \to +\infty$) underestimating the transmission coefficient by even five orders of magnitude at the lowest reported energies, with respect to the case of a Gaussian wave packet with size ξ smaller than the size of the effective well. The case of small positional variance should correspond, for a state of minimal quantum uncertainty, to a broad distribution of possible momenta, including some corresponding to kinetic energies comparable or higher than the barrier height. Notice the presence of resonant tunneling in the case of plane waves and spatially delocalized Gaussian wave packets, which is instead washed out in the integration when considering Gaussian wave packets of smaller width in position, and therefore broader in momentum/wave vector space.

In Fig. 3 we present the average reactivity corresponding to a Maxwell-Boltzmann distribution versus temperature for different values of the positional spreading ξ. Reflecting the results presented in Fig. 2, the high temperature behavior is the same for the various cases, while at low temperature the same pattern appears, with the highest reactivity occurring for the Gaussian wave packet of smallest value. Notice a further curve (dashed) which is evaluated for a temperature-dependent positional spreading as discussed in [26]. This curve is relevant for at least two reasons. First, without any active control of the positional variance of the wave packet, this is what we expect by considering a gas of reagents with a Maxwell-Boltzmann distribution. Secondly, in the temperature range between 10 keV and 100 keV, of interest for controlled thermonuclear fusion, we estimate a boost of the reactivities if compared to the ones achieved by considering plane waves. This is more easily noticeable in Fig. 4, where we report the ratio between the dashed curve of Fig. 3 and the curve corresponding to the prediction of plane waves, versus the temperature. In the above mentioned range the ratio is about 1.5, followed by a mild increase to almost 2, then becoming smaller than unity at even higher temperatures. The peak value of the ratio depends on the involved masses, as shown in the comparison of the two nucleons with a mass of 2 a.m.u. (reduced mass of 1 a.m.u.) and 12 a.m.u. (reduced mass of 6 a.m.u.). While the latter example has been chosen having in mind the case of Carbon quite relevant in astrophysics, it should be kept in mind that the same GWS potential is used in both cases to see the sole dependence on the mass, which is unrealistic for Carbon especially in regard to its actual larger well width.

We emphasize more these considerations from a complementary standpoint by plotting the reactivity as a function of the positional variance ξ for values of temperature relevant to fusion processes of light nuclei, $\beta^{-1} = 10, 20, 50, 100$ keV, as depicted in Fig. 5. This plot allows to better appreciate that there is an optimal value of ξ maximizing the reactivity at a given temperature. Indeed, in the case of $\xi \to 0$ there will be increasing components of the wave packet at large k. These components will saturate the transmission coefficient to its maximum value, and will strongly suppress the cross-section due to the dependence of the latter upon $1/k^2$, with the overall dependence on reactivity then scaling as the inverse of the wave vector.

The above results have been tested for various choices of the parameters of the potential with outcome qualitatively similar to the specific case considered in this paper. We expect robustness also in the case of a potential which is the sum of a flat potential at distances smaller than the average radius of the nuclei, and a Coulomb potential. The outcome should also hold in the more realistic three-dimensional setting, when including effects due to the angular momentum, and a spherically symmetric electric field inside the nucleus assuming uniform electric charge density. Indeed, intuitively, in the full three-dimensional case the scattering of plane waves as initial states is expected to differ even more from the case of initial states well localized in position, and the thermal distribution of K will be proportional to $K^2 \exp(-\beta\hbar^2 K^2/(2m))$. However, more extensive analyses will be necessary to determine the quantitative gain in using optimized Gaussian wave packets under these more realistic – yet not susceptible of analytic solutions – situations.

4. Conclusions

In conclusion, we have investigated the sensitivity of tunneling processes to the preparation of Gaussian wave packets – and contrasted to the usually assumed case of plane waves – in the case of an analytically solvable potential and in the presence of a canonical ensemble of nuclei. Two sources of uncertainty in the knowledge of the wave vector are present, the quantum mechanical uncertainty due to the consideration of a wave packet of positional spread ξ instead of a plane wave, and the classical uncertainty in the energy of the particle belonging to an ensemble with an energy distribution given by classical statistical mechanics. In the specific case of Gaussian wave packets and a canonical distribution, the two sources of uncertainty are combined in a simple formula leading to a positional spreading as in Eq. (9), which can also be interpreted as a positional spreading renormalized by the presence of the environment of surrounding nuclei at finite temperature. We have evidenced sensitivity of the resulting reactivities for fusion processes, a result of interest also in the astrophysical setting for primordial nucleosynthesis [28]. It is still unclear how to engineer in general wave packets of well-defined, targeted, positional variance. These results should provide further stimuli to design thermonuclear fusion prototypes in which emphasis is put in maximizing the plasma temperature with more moderate plasma density, an important point for achieving deuterium-deuterium fusion, with well-known advantages with respect to the currently experimentally investigated deuterium-tritium fusion [29].

Declaration of competing interest

The authors declare that they have no known competing financial interests or personal relationships that could have appeared to influence the work reported in this paper.

Data availability

Data will be made available on request.

References

[1] L. Esaki, New phenomenon in narrow germanium p-n junctions, Phys. Rev. 109 (1958) 603–604.
[2] F.T. Vasko, A.V. Kuznetsov, Tunneling in heterostructures, in: Electronic States and Optical Transitions in Semiconductor Heterostructures, in: Graduate Texts in Contemporary Physics, Springer, New York, NY, 1999.
[3] G. Gamow, Zur Quantentheorie der Atomkernes, Z. Phys. 51 (1928) 204–212.
[4] R.W. Gurney, E.U. Condon, Quantum mechanics and radiactive disintegration, Nature 122 (1928) 439; Phys. Rev. 33 (1929) 127–140.
[5] E.G. Adelberger, et al., Solar fusion cross-sections, Rev. Mod. Phys. 70 (1998) 1265–1291.
[6] D. Atkatz, H. Pagels, Origin of the Universe as a quantum tunneling event, Phys. Rev. D 25 (1982) 2065–2073.
[7] A.B. Balantekin, N. Takigawa, Quantum tunneling in nuclear fusion, Rev. Mod. Phys. 70 (1998) 77–100.
[8] R. Vanderbosch, Angular momentum distributions in subbarrier fusion reactions, Annu. Rev. Nucl. Part. Sci. 42 (1992) 447–481.
[9] M. Beckerman, Sub-barrier fusion of two nuclei, Rep. Prog. Phys. 51 (1988) 1047–1103.
[10] K. Hagino, Sub-barrier fusion reactions, Contribution, in: I. Tanihata, H. Toki, T. Kajino (Eds.), Handbook of Nuclear Physics, Springer, 2022, arXiv:2201.08061.
[11] L.A. MacColl, Note on the transmission and reflection of wave packets by potential barriers, Phys. Rev. 40 (1932) 621–626.
[12] B.B. Kadomtsev, M.B. Kadomtsev, Wavefunctions of gas atoms, Phys. Lett. A 225 (1997) 303–310.
[13] L.C. Vaz, J.M. Alexander, G.R. Satchler, Fusion barriers, empirical and theoretical: evidence for dynamics deformation in subbarrier fusion, Phys. Rep. 69 (1981) 373–399.
[14] V.V. Dodonov, A.B. Klimov, V.I. Man'ko, Low energy wave packet tunneling from a parabolic potential well through a high potential barrier, Phys. Lett. A 22 (1996) 41–48.
[15] M.A. Andreata, V.V. Dodonov, Tunneling of narrow Gaussian packets through delta potentials, J. Phys. A, Math. Gen. 37 (2004) 2423–2438.
[16] A.V. Dodonov, V.V. Dodonov, Tunneling of slow quantum packets through the high Coulomb barrier, Phys. Lett. A 378 (2014) 1071–1073.
[17] V.V. Dodonov, A.V. Dodonov, Transmission of correlated Gaussian packets through a delta-potential, J. Russ. Laser Res. 35 (2014) 39–46.
[18] C. Rubbia, Particle accelerator developments and their applicability to ignition devices for intertial fusion, Nucl. Instrum. Methods Phys. Res., Sect. A 278 (1989) 253–265.
[19] K.-F. Liu, A. Chao, Accelerator based fusion reactor, Nucl. Fusion 57 (2017) 084002.
[20] B.C. Lutfuğlu, F. Akdeniz, O. Bayrak, Scattering, bound, and quasi-bound states of the generalized symmetric Woods-Saxon potential, J. Math. Phys. 57 (2016) 032103.
[21] A. Arda, O. Aydoğdu, R. Sever, Scattering of the Woods-Saxon potential in the Schroedinger equation, J. Phys. A, Math. Theor. 43 (2010) 425204.
[22] S. Kimura, N. Takigawa, Fusion from an excited state, Phys. Rev. C 66 (2002) 024603.
[23] W. Voigt, Uber das Gesetz der Intensitatsverteilung innerhalb der Linien eines Gassperktrums, in: Sitzungsbericht der Bayerischen Akademie der Wissenschaften, vol. 25, 1912, pp. 603–620.
[24] B.H. Armstrong, Spectrum line profiles: the Voigt function, J. Quant. Spectrosc. Radiat. Transf. 7 (1967) 61–88.
[25] G.R. Satchler, Introduction to Nuclear Reactions, Palgrave, Macmillan, London, 1990.
[26] A. Chenu, M. Combescot, Many-body formalism for thermally excited wave packets: a way to connect the quantum regime to the classical regime, Phys. Rev. A 95 (2017) 062124.
[27] S. Alterman, J. Choi, R. Durst, S.M. Fleming, W.K. Wootters, The Boltzmann distribution and the quantum-classical correspondence, J. Phys. A, Math. Theor. 51 (2018) 345301.
[28] R. Bonetti, et al., First measurement of the ^{3}He(^{3}He, 2p)^{4}He cross section down to the lower edge of the solar Gamow peak, Phys. Rev. Lett. 82 (1999) 5205–5208.
[29] R. Onofrio, Concepts for a deuterium-deuterium fusion reactor, J. Exp. Theor. Phys. 127 (2018) 883–888.